Change of mechanical properties of AM60B alloy with heat treatments and its correlation with small punch tests

Pedro Miguel Bravo Díez , Monica Preciado Calzada, David Cárdenas Gonzalo, José Calaf Chica

Departamento de Ingeniería Civil (Universidad de Burgos), Calle Villadiego s/n, 09001 Burgos, Spain

a r t i c l e i n f o

Article history:
Received 30 June 2016
Revised 15 September 2016
Accepted 27 September 2016 Available online 28 September 2016

Keywords:
AM60B
AZ91D
Small punch test
High pressure die casting
Squeeze casting
Heat treatments

a b s t r a c t

AM60B alloy, injected by high pressure die casting process (HPDC), is one of the most widely used alloys for its ease of processing and low price. There is an industrial interest in the use of heat treatments in order to increase the elongation before failure of the alloy. This paper aims to correlate the results of tensile test of heat treated specimens with small punch tests (SPT's). It is also intended to find out if the different characteristic values of such tests for different mechanical properties are sensitive enough to detect changes produced by heat treatments or injection process parameters and if the correlation factors are sufficiently stable. In addition, this study is also focused on the validation of the applicability of such miniature tests for high pressure die casting magnesium alloys, since this process introduces a significant number of defects and thus a variability of the mechanical properties is expected.

1. Introduction

Magnesium alloys injected at high pressure are of great industrial interest because of their price and ease of processing. The magnesium alloys most commonly used for high pressure die casting (HPDC) are the AM60B alloy and AZ91D alloy. AM60B alloy has a moderate resistance at room temperature and greater ease of processing and ductility than AZ91D alloy, with AZ91D alloy having a higher specific resistance but lower ductility due to its higher aluminum content.

It is of great interest to the industry to improve injection processes and use thermal treatments to increase the capacity of plastic deformation and consequently the energy absorption capacity. In this aspect porosity is a drawback.

In recent years there have been many studies on the application of the miniature punch test (SPT – Small punch test) for alloys. In these studies, the values of mechanical properties obtained by tensile tests are correlated with the characteristic values of the miniature punch tests, subsequently allowing expressions which predict the mechanical properties when only miniature punch tests are performed. These tests are used to predict properties such as the tensile strength and elongation at break [1–3], creep [4] and fracture toughness [5,6], as well as others.

Furthermore, studies have also been done using miniature punching shear tests for AM60B alloy in which the maximum strength and the elastic limit of tensile test and punching shear tests have been correlated [7], in addition to hardness and maximum strength [8].

This paper presents the correlation between the results of tensile test specimens and SPT's for magnesium alloys AM60B and AZ91D injected using HPDC (High Pressure Die Casting) and alloy AM60B injected using ''Squeeze Casting", with and without heat treatment. Specimens of the AM60B alloy injected by a process of ''Squeeze Casting" (high-pressure injection with a final stage of mechanical compaction) were tested, since this process reduces the inherent porosity of the classic HPDC injection and thus improves elongation at break and could allow for the introduction of heat treatments.

On the one hand, it is intended to see if the characteristic values of such tests (SPT) for different mechanical properties are sensitive enough to detect changes that occur due to the process and the thermal treatments performed and if the correlation factors are sufficiently stable. On the other hand, it is aimed validating the applicability of SPT to HPDC magnesium alloys, since the process introduces a significant number of defects and consequently a variability of the mechanical properties.

Fig. 1 shows the typical load-displacement curve of a small punch test for AM60B alloy manufactured by ''Squeeze Casting"

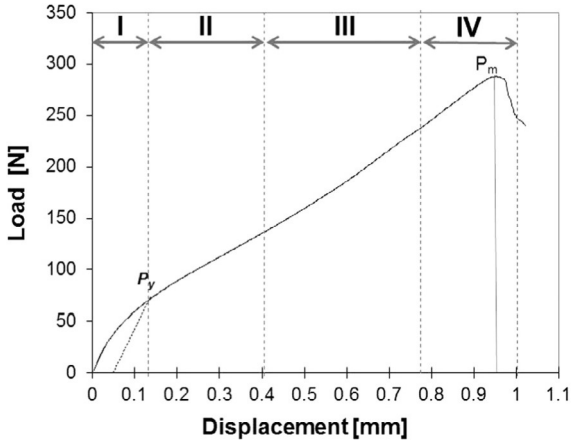

Fig. 1. Characteristic curve of Small Punch Test (SPT) for the alloy AM60B ''Squeeze Casting".

Corresponding author.

E-mail addresses: pmbravo@ubu.es (P.M. Bravo Díez), mpreciado@ubu.es (M. Preciado Calzada), dcardenas@ubu.es (D. Cárdenas Gonzalo), jcc0087@alu. ubu.es (J. Calaf Chica).

and its characteristic zones (zone I, II, III, IV) according to authors such as those referenced [1,3,9]. For AZ91D and AM60B alloys injected at high pressure (HPDC), the inflection point limiting zones II and III is not present or is not well defined in their SPT test curves because of their lesser elongation at break.

Although there are other factors, undoubtedly the thickness of the specimen is one of the parameters that most influences the load-displacement values of SPT's [10]. In the particular case of this study, the thickness of the SPT specimens was between 0.495 and 0.505 mm, as recommended [10].

One of the decisions to be made is the choice of the load P_y, limiting zones I and II of the curve. This value divided by the initial SPT specimen thickness squared t^2 has to be correlated to the material yield strength r_y. Such relationship is shown by expressions like:

$$\sigma_y = \alpha \frac{P_y}{t^2} \quad (1)$$

$$\sigma_y = \alpha_1 \frac{P_y}{t^2} + \alpha_2 \quad (2)$$

t

where a, a_1 and a_2 are correlation parameters.

Correlations between maximum tensile strength r_{max} maximum load P_m and are shown by the following expressions:

$$\sigma_{max} = \beta \frac{P_m}{t^2} \quad (3)$$

$$\sigma_{max} = \beta_1 \frac{P_m}{t^2} + \beta_2 \quad (4)$$

where b_1 and b_2 are correlation coefficients.

And to estimate the elongation under maximum load A_{gt} the expression used is: d_m

$$A_{gt}\ (\%) = \gamma_1 \frac{d_m}{t} + \gamma_2 \quad (5)$$

where d_m is the displacement under maximum load in the SPT, c_1 and c_2 are correlation coefficients.

In this paper, the calculation of P_y taking into account the code of good practice [10], which it is based on the calculation of the vertical projection of the point of intersection of the tangents on

Table 1

the curve test, does not provide reliable data for alloys injected using HPDC, so this method was not selected. The method used for calculating P_y is the intersection of the curve with a line parallel to the elastic zone displaced a value of 1/10 times the initial thickness of the specimen (see Fig. 1) [11,12].

2. Materials and experimental methodology

2.1. Materials

The materials used for this study were:

AM60B alloy injected using HPDC.

AZ91D alloy injected using HPDC.

AM60B alloy injected using ''Squeeze Casting (SC)". Alloy AM60B injected using SC and with a 4-h T4 treatment at 420 C.

The chemical composition of the alloys AM60B an AZ91D can be shown in Table 1.

As shown in the metallography of Fig. 2, the structure of AM60B injected using HPDC alloy has a dendritic structure, formed by magnesium in solid solution in which the aluminum content increases toward the grain boundary, and the intermetallic compound $Mg_{17}Al_{12}$ which concentrates on the grain boundaries in the form of eutectic.

Figs. 3 and 4 represent the microstructure of alloy AM60B injected using SC either without or with T4 heat treatment respectively. Comparing both images, the solution of the intermetallic compound with the heat treatment can be appreciated. The evolution of the microstructure of the AM60B injected using SC for the different solution times at 420 C at 0.5 mm from the surface is shown in Fig. 5. The differences in the microstructure from the center to the boundaries of the section are visible comparing Figs. 3 and 5(a).

The microstructure of the AZ91D alloy injected using HPDC can be observed in Fig. 6. The amount of the intermetallic compound $Mg_{17}Al_{12}$ at grain boundaries is greater due to the greater amount aluminum in its chemical composition.

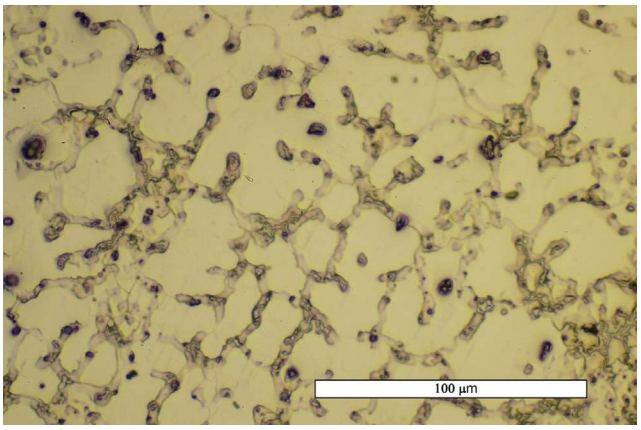

Fig. 2. Microstructure of the AM60B HPDC alloy. 400X Etch: Acetic glycol.

Chemical composition for magnesium alloy die-castings AM60B and AZ91D according to ASTM B94[15].

Designation	UNS	Al	Mn	Zn	Cu max	Fe max	Si	Ni	Other met. impurities max
AM60B	M10602	5.5–6.5	0.24–0.6	0.22	0.010	0.005	0.10	0.002	0.02
AZ91D	M11916	8.3–9.7	0.15–0.50	0.35–1.0	0.030	0.005	0.10	0.002	0.02

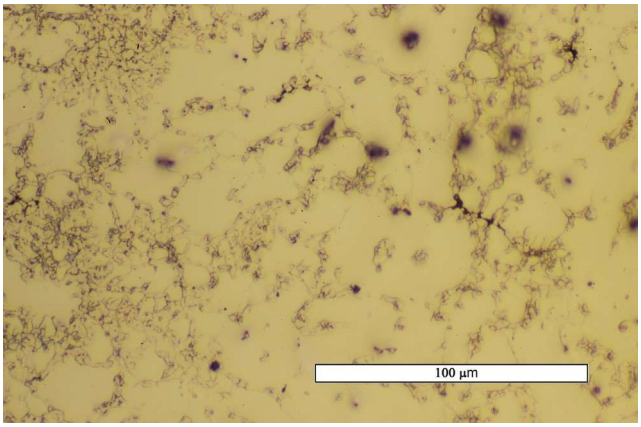

Fig. 3. Microstructure of the AM60B-SC alloy as cast. Center. Etch: Acetic glycol.

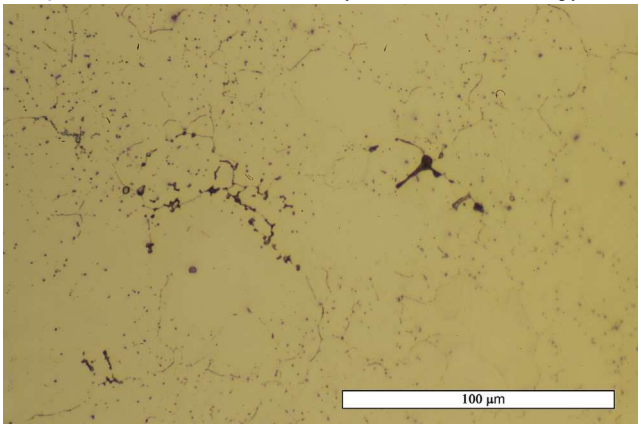

Fig. 4. Microstructure of the AM60B-SC alloy with a 4-h T4 treatment at 420 C. Etch: Acetic glycol.

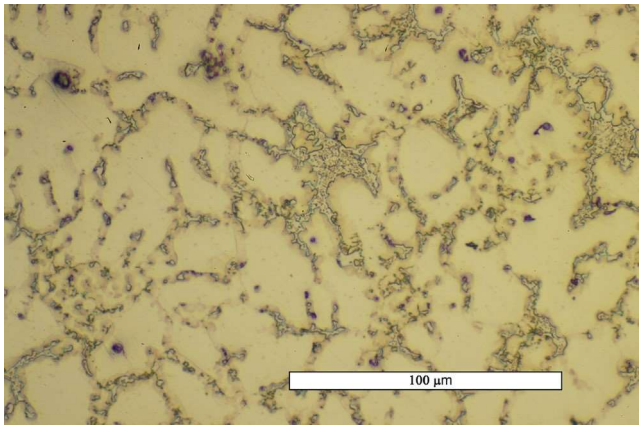

Fig. 6. Microstructure of the AZ91D HPDC alloy. Etch: Acetic glycol.

2.2. Experimental methodology

Conventional tensile test specimens were used for the material characterization. These specimens were obtained by injection under high pressure into a mold with the final geometry (Fig. 7). Small punch test specimens were made by first cutting slides from the calibrated zone of the injected tensile test specimens for the different materials tested and then grinding until their final thickness. SPT specimens had a nominal thickness of 0.5 mm as directed [10]. The diameters of the samples varied between 6.4 and 6.5 mm depending on the diameters of the calibrated zones of the specimens from which they were extracted.

The heat treatment for AM60B alloy specimens injected using ‘‘Squeeze Casting” was performed in a Carbolite 1300 CWF oven without inert atmosphere for 4 h at 420 C and then water quenched. The choice of the heat treatment solution time was based on the evolution of hardness for specimens treated for 1 h, 2 h, 4 h and 8 h at surface distances of about 0.5, 1 and 3.2 mm (center of the diameter). Hardness HV500 test results were obtained from single indentations at theses depths.

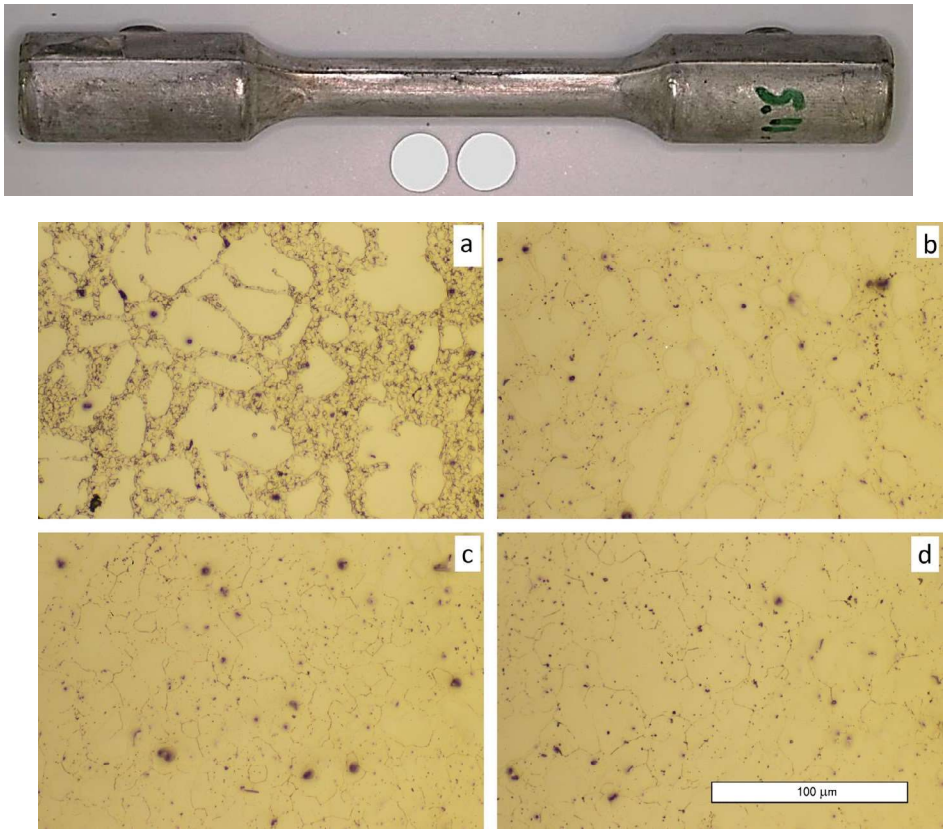

Fig. 5. Evolution of the microstructure of the AM60B-SC alloy with T4 heat treatment time at 420 C. Etch: Acetic glycol. (a) As cast, (b) T4-1 h, (c) T4-2 h, and (d) T4-4 h.

Fig. 7. Specimens for tensile test and SPT's.

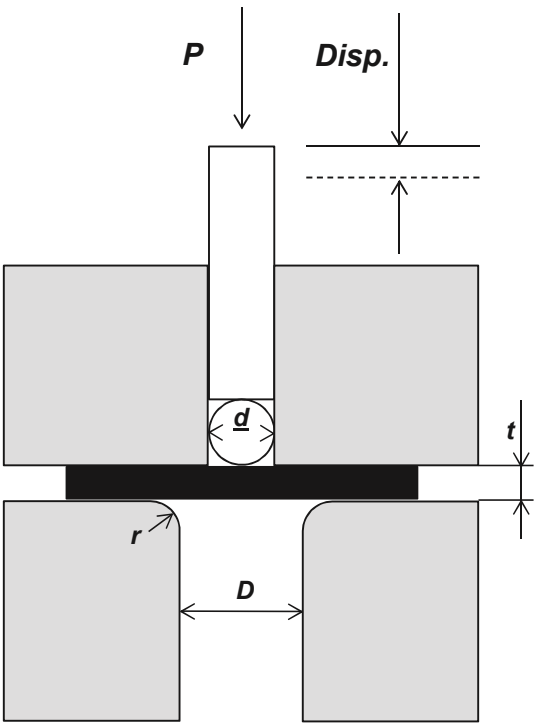

Fig. 8. SPT outline.

The hardness evolution is due to the dissolution of the phase $Mg_{17}Al_{12}$, the homogenization of the composition of the a phase and grain growth (see Figs. 4 and 5). Apparently, according to the results of hardness tests, homogeneity level is reached within four hours of treatment, so this amount of time was chosen.

Tensile tests according to standard [13] and SPT's according to the code of good practice [10] were performed on a Zwick/Roell DS 050 KAPPA machine with a 50 kN load cell and a 1 kN load cell respectively. An outline of the testing die for the SPT is shown in Fig. 8. The diameter of the loading ball d was 2.5 mm, the diameter of the lower die D was 4 mm, and the corner radius r was 0.5 mm. A constant loading speed of 0.5 mm/min was used.

The evaluation of results from load-displacement SPT curves were done according to the methodology proposed by accepted studies [1,3,9]. The chosen limit between curve zones I and II was $P_{y\_t/10}$.

Fig. 14 shows SPT load-displacement curves for the four materials. For AZ91D HPDC material, the points taken as maximum load and maximum displacement correspond to the maximum load of the first peak of the SPT curve, since from that point breakage begins (see detail in Fig. 14). After that point, cracks propagate until the end of the test. Interrupted tests were done to see when cracking was started. For other materials, the maximum load point of each test and its corresponding displacement were taken.

The macroscopic aspect of the SPT specimens varies progressively from the AZ91D HPDC material having the most brittle behavior to the AM60B SC + T4 materials having the most ductile behavior (Fig. 15).

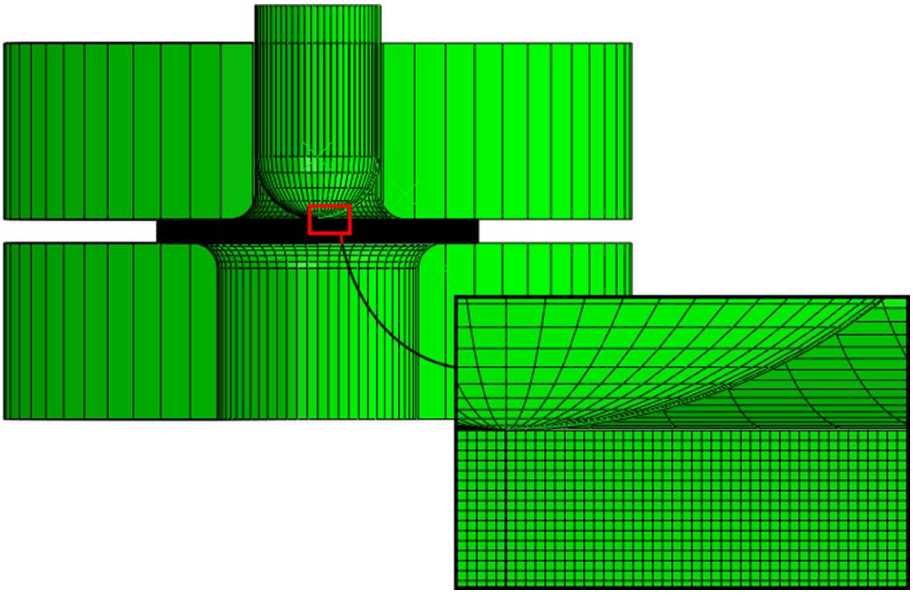

Fig. 9. FE model of Small Punch Test.

2.3. Influence of the diameter of the SPT specimens

The diameter of the tensile test specimens of approximately 6.5 mm is a typical value used for this materials and the obtained microstructure is representative for parts made of magnesium alloys injected using HPDC. A centering plate with a thickness of 0.3 mm and with a circular hole of 6.6 mm was used to place the SPT specimens in a correct position before running the test. As specified in the code of good practice [10], the recommended diameter for the test sample should be equal to 8.0 mm. An exploration of the influence of the specimen's diameter was made through a finite element (FE) analysis to make sure that these diameters were suitable and had no significant influence in SPT load/displacement curve.

Alloy AM60SC + T4 was selected to perform this study because of its greater elongation at brake. Elastic modulus and plastic behavior was taken and tabulated from the tensile test curve and then introduced in the FE model. No damage model was introduced in the FE model.

Abaqus/Standard software was used to perform this analysis, taking advantage of the axisymmetric geometry of the SPT to simplify the FE model. Considering the low load level of SPT's and the lower mechanical characteristics of the tested magnesium alloys compared to steel, steel parts (upper and lower dies and spherical puncher) were considered as rigid surfaces without a significant influence in the SPT load/displacement curve.

CAX4R elements (axisymmetric quadrilateral elements with reduced integration and hourglass control) with a length of 0.02 mm were selected to mesh the test sample. Fig. 9 shows the FE model. For all contact surfaces, a friction coefficient equal to $\mu = 0.1$ was established. To simulate the tightening effect of upper and lower dies, an initial forced displacement of the lower die was performed generating a pre-stress of 1200 N (the load considered due to the applied torque in the assembly of the experiment).

Fig. 10 shows the load/displacement SPT results of the FE model with test sample diameters of 6.5 mm and 8.0 mm. Experimental results have also been included to show the consistency of the FE model results. Curves for both diameters match up with each other and with the experimental curve, so test sample diameter of 6.5 mm could be considered to have the same behavior in a small punch test as a test sample diameter of 8.0 mm. It is important to note that this conclusion applies only for the SPT load range and materials shown in this analysis. Other load ranges or materials could show other behaviors.

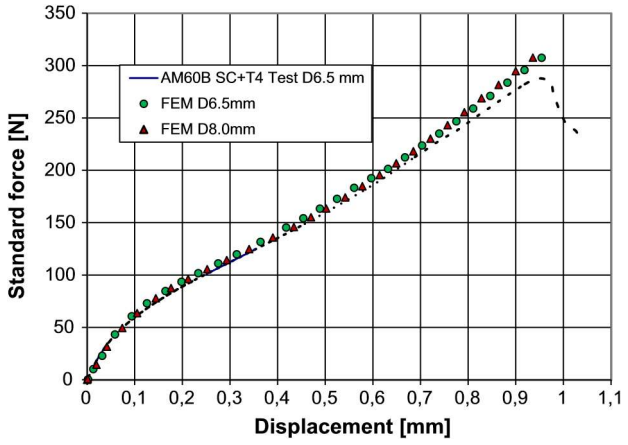

Fig. 10. FEM and experimental load-displacement curves with different sample diameter.

It can be deduced from above that for the materials used in this study and in the conditions that have been tested, there is no significant influence from the specimen's diameter in the SPT test results.

3. Results and discussion

3.1. Test results

In Fig. 11, hardness test results for AM60B alloy injected using SC for different times of solubilization are shown. Two important facts were observed:

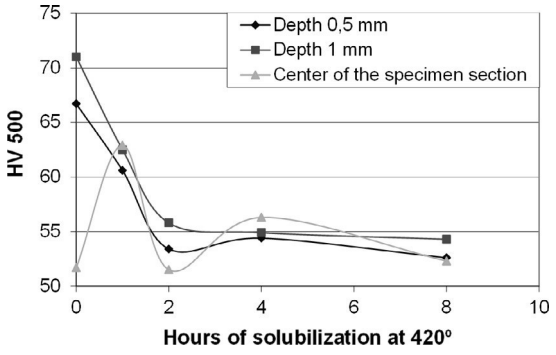

Fig. 11. Evolution of hardness at different depths depending on the time of solubilization at 420 C.

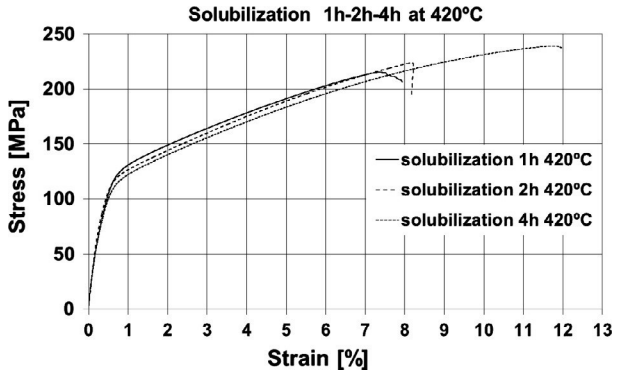

Fig. 12. Stress-strain curves for AM60B alloy with different heat treatments.

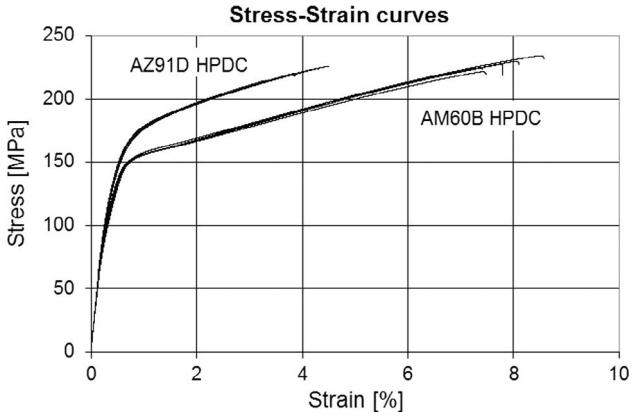

Fig. 13. Tensile test stress-strain curves for AM60B HPDC and AZ91D HPDC alloys.

For the non-heat treated material, there were important differences in hardness between the areas near the surface and the center in the specimen section. After four hours of solution treatment, an adequate level of homogeneity was obtained.

Tensile tests were performed on specimens with solubilization treatments of 1 h, 2 h and 4 h. A marked increase in elongation at break was observed for specimens with the 4 h solubilization treatment as shown in Fig. 12. Based on these results, the T4 condition of 4 h at 420 C for AM60B alloy injected using SC was selected.

Fig. 13 shows the results of tensile tests conducted on alloys AM60B HPDC and AZ91D HPDC in which it can be observed how AZ91D alloy has a higher yield strength and a lesser elongation at break.

The average values of the results obtained in tensile tests for the different materials used in this work are shown in Table 2. Five tests were performed for each material.

In Table 3 the average values of the results obtained in SPT's for the four materials tested are shown. A minimum of three tests were performed for each material.

3.2. Correlation between the tensile tests and SPT's

For the AZ91D alloy, the reference value P_{y_CEN} could not be determined because the test curve did not become linear in zone

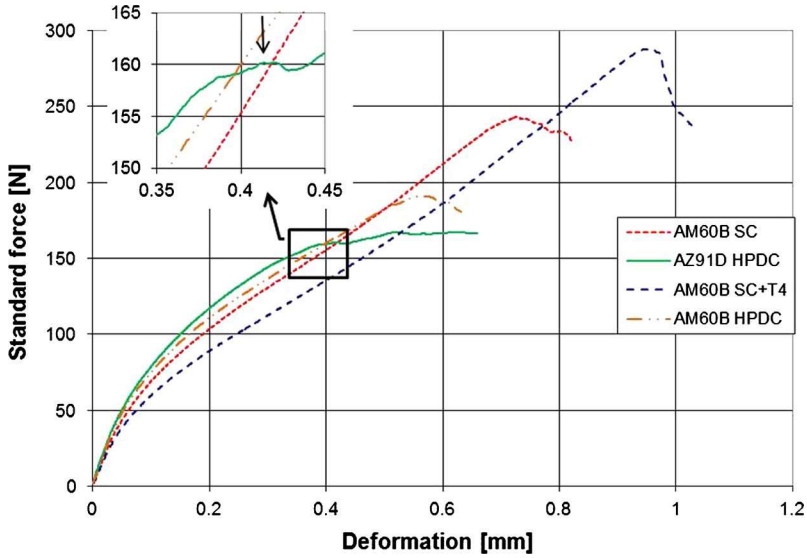

Fig. 14. SPT curves for the four materials considered. In the detail, the first maximum point considered for the AZ91D HPDC material to correlate with the maximum strength of tensile tests can be observed.

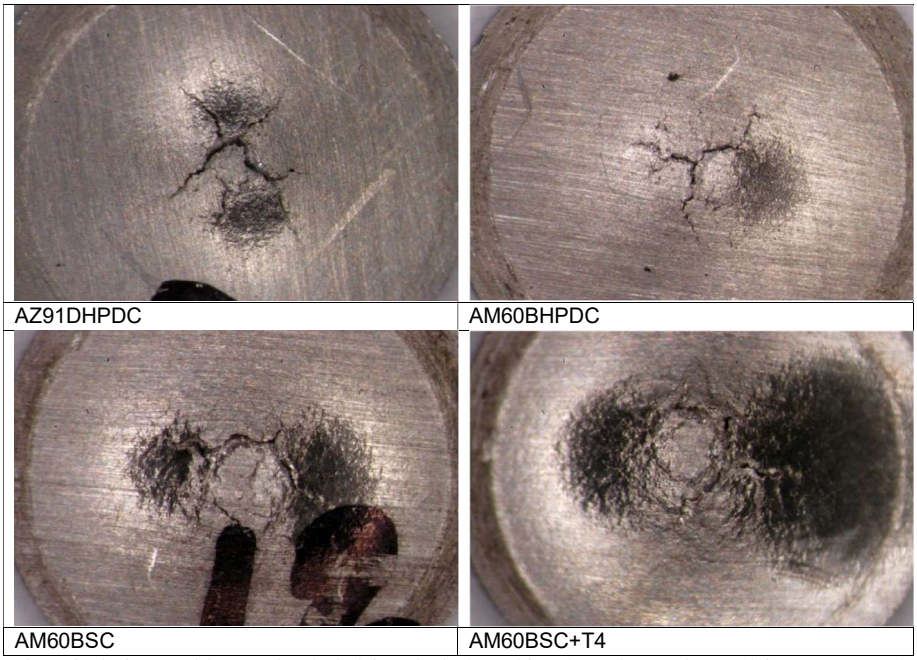

Fig. 15. Macrographs of the SPT specimens for the four materials. Increasing plastic deformation is observed from the specimen on the upper left corner to one on the lower right corner.

Table 2
Characteristic values of the tensile tests for the tested materials.

Material		$Rp_{0.2}$ (MPa)	R_m (MPa)	A_{gt} (%)
AM60B SC	Mean Val. St.	133	212	6.5
	Dev.	8.1	5.3	0.54
AM60B SC + T4	Mean Val. St.	106 1.5	241	11.7
	Dev.	138	2.8	0.2
AM60B HPDC	Mean Val. St.	1.2	227	7.8
	Dev.	153	4.7	7.8
AZ91D HPDC	Mean Val.	2.3	221	4.0
	St. Dev.		4.4	0.46

Table 3
Characteristic values of SPT's for the materials tested.

Material		$P_{y\_t/10}$ (N)	P_{y_CEN} (N)	d_m (mm)	P_m (N)
AM60B SC	Mean Val.	82.7	58.5	0.75	239
	St. Dev.	1.3	0.38	0.08	28.2
AM60B SC + T4	Mean Val.	71.7	51.3	1.02	306
	St. Dev.	5.8	3.6	0.07	24.2
AM60B HPDC	Mean Val.	87.6	62.4	0.66	211
	St. Dev.	3.8	3.4	0.07	15.3
AZ91D HPDC	Mean Val.	95.3	–	0.40[a]	162[a]
	St. Dev.	0.85	–	0.03	7.8

[a] Values for the maximum load and displacement of the first peak of the curve.

II. Accordingly, the value of $P_{y\_t/10}$ instead of P_{y_CEN} was used when establishing correlations between the characteristic values of SPT and tensile tests.

Graphs in Figs. 16 and 17 show the correlation between r_{max} with P_m and A_{gt} with d_m respectively. It is clearly seen in both cases how the point corresponding to the alloy AM60B SC (not heat treated) remains away from the line marked by the others points. The cause that justifies such deviation is the high anisotropy between the center and the surface of the calibrated section area. As mentioned, this anisotropy is identified by differences in

Table 4
Approaches selected to evaluate material properties from SPT's results.

Yield strength σ_y (MPa)	Maximum strength σ_{max} (MPa)	Agt (%)	Ref
$\sigma_y = 0{:}346\frac{P_{y\_t/10}}{t^2}$	$\sigma_{max} = 0{:}277\frac{P_m}{d_m t}$	$A_{gt}\ (\%) = 6{:}07\frac{d_m}{t}$	[14]
$\sigma_y = 0{:}3417\frac{P_{y\_t/10}}{t^2}$ 10:36	$\sigma_{max} = 0{:}080\frac{P_m}{t^2} + 22{:}44$	$A_{gt}\ (\%) = 6{:}04\frac{d_m}{t} + 0{:}94$	[3]

hardness between the center and the surface of the calibrated section area of the specimen.

The SPT only affects the central area of the specimen section which has lower hardness and greater elongation than the surface of the section, whereas the tensile test obtains average values for the sample section. Therefore, both values load and maximum elongation for this point move to the right of the trend line in the corresponding graphs.

This anisotropy is less obvious in Fig. 18 where the yield stress σ_y is correlated with the load P_y for SPT's, but it can be explained in the same way. The yield stress in the center of the specimen section corresponding to the AM60B alloy SC is lower than the yield stress close to the surface of the section and thus lower than that of the whole

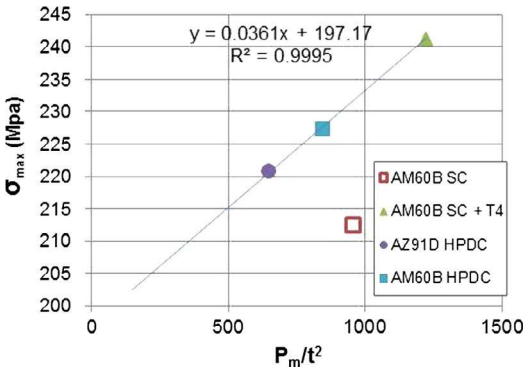

Fig. 16. Correlation between maximum strength σ_{max} and maximum load P_m.

specimen. Hence, the point for this alloy represented in Fig. 18 moves leftwards. Based on these arguments, the decision not to include this item for setting the correlations in all cases was taken.

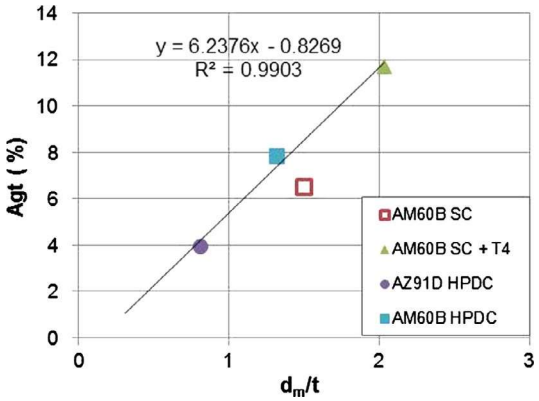

Fig. 17. Correlation between elongation under maximum load A_{gt} for tensile tests and displacement under maximum load d_m for SPT's.

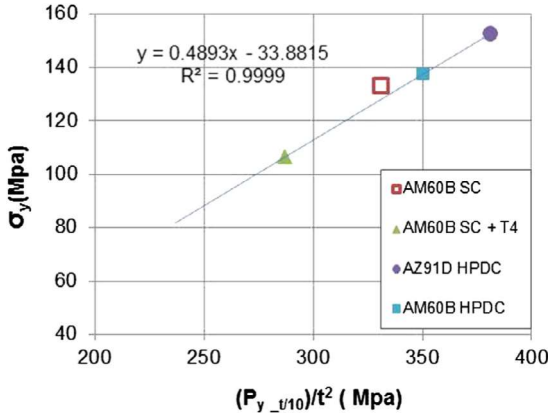

Fig. 18. Correlation between yield stress σ_y and load P_y.

Eq. (2) was used to calculate the correlation coefficients between σ_y and P_y. The obtained values were $a_1 = 0{:}4893$ and $a_2 = 33{:}882$.

And Eq. (4) was used to obtain the correlation coefficients between the maximum resistance σ_{max} and maximum load of SPT test, P_m. The obtained values were $b_1 = 0{:}0361$ and $b_2 = 197{:}17$.

Eq. (5) was used to obtain the correlation coefficients between the elongation under maximum load A_{gt} and the displacement at maximum load of SPT d_m. Values of $c_1 = 6{:}2376$ and $c_2 = 0{:}8269$ were obtained.

3.3. Comparison with other approaches

Approaches obtained by Rodriguez et al. [3] for different grade steels are similar to those obtained in this study for Eqs. (2), (4), and (5) (see Table 4).

Approaches from Garcia et al. [14] obtained for equations listed in Table 4 give good results in the prediction of the properties for the magnesium alloys.

4. Conclusions

Very good correlations were obtained in the implementation of SPT's versus tensile tests for magnesium alloys injected at high pressure.

The Small Punch Test is able to show the changes that are produced by different injection processes on the mechanical properties of the injected alloy, as well as changes produced by heat treatments. The SPT also reveals changes in mechanical properties due to the composition of the alloy like with HPDC AZ91D alloy with respect to HPDC AM60B alloy.

It has been shown that the use of SPT specimens, obtained from the calibrated zone of the tensile test specimens injected at high pressure and with lower diameters than those recommended by the code, are effective when reproducing the mechanical properties of the alloy, provided that the section is sufficiently uniform in mechanical properties.

Local anisotropy, as in the case of SC AM60B alloy, can produce a significant deviation of SPT results from those obtained in tensile tests. However, this opens a way for the study of the evolution of the mechanical properties in different points of molded parts and along the thickness of their walls.

References

[1] I.I. Cuesta, J.M. Alegre, Hardening evaluation of stamped aluminum alloy components using the small punch test, Eng. Fail. Anal. 26 (2012) 240–246.

[2] Y.W. Ma, K.B. Yoon, Assessment of tensile strength using small punch test for transversely isotropic aluminum 2024 alloy produced by equal channel angular pressing, Mater. Sci. Eng. 527 (2010) 3630–3638.

[3] C. Rodriguez, T.E. Garcia, F.J. Belzunce, I. Penuelas, The Application of the Small Punch Test to the Mechanical Characterization of Different Steel Grades, Ocelot Sro, Ostrava, 2012.

[4] S. Yang, X. Ling, Y. Zheng, R. Ma, Creep life analysis by an energy model of small punch creep test, Mater. Des. 91 (2015) 98–103.

[5] T.E. Garcia, C. Rodriguez, F.J. Belzunce, I.I. Cuesta, Development of a new methodology for estimating the CTOD of structural steels using the small punch test, Eng. Fail. Anal. 50 (2015) 88–99.

[6] R. Lacalle, J.A. Álvarez, T.E. García, F. Gutiérrez-Solana, Estimación de la Tenacidad a la Fractura mediante probetas a partir de probetas Small Punch entalladas, Anales de Mecánica de la Fractura 25 (2008).

[7] F. Akbaripanah, F. Fereshteh-Saniee, R. Mahmudi, H.K. Kim, Microstructural homogeneity, texture, tensile and shear behavior of AM60 magnesium alloy produced by extrusion and equal channel angular pressing, Mater. Des. 43 (2013) 31–39.

[8] B. Kondori, R. Mahmudi, Effect of Ca additions on the microstructure, thermal stability and mechanical properties of a cast AM60 magnesium alloy, Mater. Sci. Eng. 527 (2009) 2014–2021.

[9] R. Lacalle, J.A. Alvarez, F. Gutierrez-Solana, Analysis of key factors for the interpretation of small punch test results, Fatigue Fract. Eng. Mater. Struct. 31 (2008) 841–849.

[10] CEN Workshop Agreement, Small Punch Test Method for Metallic Materials, European Committee for Standardization, 2006.

[11] J. Autillo, M.A. Contreras, C. Betegón, C. Rodríguez, F.J. Belzunce, Utilización del ensayo miniatura de punzonamiento (small punch test) en la caracterización mecánica de aceros, Anales de Mecánica de Fractura 23 (2006).

[12] C. Rodríguez, T.E. García, E. Cárdenas, F.J. Belzunce, C. Betegón, Mechanical properties characterization of heat-affected zone using the small punch test, Weld. J. 88 (2009) 188–192.

[13] UNE-EN-ISO-6892-1. Materiales metálicos. Ensayos de tracción. Parte 1: Método de ensayo a temperatura ambiente., AENOR ed., 2010.

[14] T.E. Garcia, C. Rodriguez, F.J. Belzunce, C. Suarez, Estimation of the mechanical properties of metallic materials by means of the small punch test, J. Alloy. Compd. 582 (2014) 708–717.

[15] ASTM B94-05. Standard specification for magnesium-alloy die castings, in: ASTM International, 2005.